

FORCE FIELD CALCULATIONS ON LINEAR POLYPYRROLE SYSTEMS

H. FALK* and N. MÜLLER

Institute of Analytical, Organic and Physical Chemistry, Johannes Kepler University, Linz, A-4040, Austria

(Received in U.K. 25 February 1982)

Abstract A force field model constructed for the conformational analysis of polypyrrolic systems is reviewed. Results are discussed and compared to experimental data where available for dipyrrolic compounds such as pyrromethenes, dipyrromethanes and pyrromethenones, for tripyrrins and for various verdinoid and rubinoid bile pigments.

LINEAR polypyrroles are important compounds not only in the path of physiological porphyrin degradation¹ but they also serve as antenna pigments for solar energy conversion in certain algae² and as photoreceptors for photomorphogenesis in the plant kingdom.³ As structure and mechanism in such natural systems can be only studied on the basis of a profound knowledge of the chemistry of linear polypyrroles (i.e. structure, reactivity, photochemistry, spectral properties) the renaissance of investigations in this field starting about ten years ago is understandable.⁴ The structural and energetic details of conformation and configuration of these compounds are of especial interest in this connection. Experimental methods for structural studies of this kind in solution are rare and an overall picture can only be obtained by using the information from several methods. It therefore seemed worthwhile to resort to methods of the *a priori* type.

In principle there are two such *a priori* methods available which yield geometry and energy of molecular states: first, the more or less sophisticated semi-empirical quantum chemical calculations⁵ where the interaction of kernels and electrons determine structural features; and second, self-consistent force field calculations⁶ based on classical mechanics and electrostatics.

Both methods have been applied to polypyrrolic compounds. They each have certain merits for solving specific problems and the first one is limited to rather small molecules and rather small parts of the energy hypersurface. For example, CNDO/2 calculations yielded very accurate information on conformation and energetic details of pyrromethenes⁷ and dipyrromethanes⁸ while MINDO/3 calculations provided results on dipole moments and structural details of pyrroles and pyrrolinones⁹ which represent the terminal rings of bile pigments. Many degrees of sophistication are possible for force field calculations they may easily be tailored to specific needs and moreover they are extremely conceptual. Therefore a force field model has been constructed for the analysis of geometry and energy of polypyrrolic compounds.

A force field model for linear polypyrrolic compounds

Besides a mechanical model consisting of springs,¹⁰ and two more or less qualitative calculations¹¹ no systematic force field investigations on pyrrolic compounds has been published before our series of papers.^{9,12-14}

Following the philosophy of force field calculations^{6,15} the total energy of a given molecular state is

set up as a sum of contributions from non-bonded interactions, deformations of standard bond lengths, bonding angles and torsional angles, interactions of permanent dipole moments, hydrogen bonding systems and conjugative stabilization. This total energy may then be minimized with respect to the geometrical variables yielding optimum geometries. Another possibility may be to follow motional trajectories as well so that a complete energy hypersurface for a molecule may be constructed.

Application of existing force field models^{6,15} to the geometry and energy problems of linear tetrapyrrolic compounds showed that rather long calculation times were necessary to find global energy minima. Many meaningless side minima were found, and due to the need to describe geometry in terms of the individual Cartesian coordinates of every atom, the motions of interest (e.g. at the exocyclic single bonds) could not be readily isolated.⁹

The first step in constructing a force field model for conformational analysis of polypyrrolic compounds was to reduce the number of free variables. Linear polypyrroles obviously have two energetically different possibilities for intramolecular motion and equilibration of stress: the exocyclic single bonds which are flexible torsionally and with respect to bond angles; and the energetically rather "rigid" pyrrolic rings as well as bond length deformations of the attached exocyclic bonds. The energy needed to deform the latter structural elements is at least one order of magnitude higher than that necessary to change geometry for the former. Therefore the pyrrolic rings are treated as rigid systems, and only bending and torsional modes are considered possible for exocyclic bonds. This leaves a relative energy (E) for a linear polypyrrolic molecule of the form

$$E = E_b + E_{nb} + E_\pi + E_\mu + E_H \quad (1)$$

E_b is the sum of all bond angle deformations of exocyclic bonds (in-plane and out-of-plane), E_{nb} is the sum of all non-bonded interactions, E_π is a conjugation energy term stemming from the diminution of conjugation in an extended π -electron system by torsion, E_μ represents the interaction of permanent dipole moments, and E_H is the sum of energies associated with intramolecular H-bonding systems. It should be noted that the conventional term for torsional energy will not be treated explicitly but can be included into an appropriate parameterization of E_{nb} and E_π as could be shown by initial trial calculations.

The second important step was to handle the

Table 1. Normalized bond lengths and bond angles for linear polypyrroles.

Bond	Length (Å)	Bond angle	(degrees)
C-H	1.09	C-C-H	109.5
N-H	1.00	C-N-H	126.0
C-C (encocycl.)	1.43	C=C-C (endocycl.)	107.8
C-alkyl	1.53	C=C-C (exocycl.)	120.0
C=C (endocycl.)	1.37	C=C-alkyl	126.0
C=C (exocycl.)	1.37	C-C=N	107.8
C-N	1.43	C-NH-C	107.8
C=N	1.35	C=N-C	107.8
C=O	1.24	C-O-C	109.5
C-O	1.40	C=C-N	107.8

molecule in terms of internal coordinates and not Cartesian ones.

1. *Mode of calculation.* The starting geometry of a linear tetrapyrrole is first established using normalized internal coordinates (bonding distances, bonding angles) by means of an adapted COORD program.¹⁶ The torsional angles at exocyclic single bonds are set as desired, and all other torsional angles within the π -system and are set at zero. The normalized bond lengths and bond angles given in Table 1 were adapted from appropriate X-ray structural work.¹⁷⁻²⁰ For exocyclic single bonds within a π -conjugated system the length of this bond depending on the associated torsional angles is given by $L(\theta) = 1.51 - 0.08|\cos\theta|$ which is deduced from the bond length-bond order correlation from PPP-SCF-LCAO-MO-CI calculations on conjugated polypyrrolic systems.²¹ These calculations also reveal that a dihedral deformation at the adjacent single bond has only a minor effect on the length of the double bond, and this is therefore neglected in our model.

From these internal coordinates of the molecule the Cartesian coordinates of the various atoms are derived. They are used in evaluating the non-bonded, dipole-dipole and H-bond interactions. E is then calculated using Eq. (1) and the five functions (2)–(6) given in the following section. Now E is minimized with respect to bonding angles and torsional angles using a modified steepest descent method.²² In the region where minima occur interpolation with a parabolic function is possible. As an option, certain torsional angles may be kept fixed, so allowing the investigation of energy hypersurfaces for variations of those angles or trajectories. The geometrical details and the energy are the output of the calculation. To set up energy hypersurfaces the conformational space was scanned first with 20 degree increments and then with smaller increments in regions of interest.

2. *The energy functions.* The five additive energy functions for Eq. (1) are as follows:

$$E_b = K_\theta \cdot (\theta - \theta_0)^2 \quad (2)$$

The energy for deformations of normalized bonding angles θ_0 to a value of θ is given by the classical function (2).²³

Using a Buckingham potential (3)²⁴ the energies of non-bonding interactions are calculated for every set

$$E_{nb} = \frac{\epsilon}{1 - 6/\alpha} \cdot [(6/\alpha) \cdot e^{\alpha(1-r/r_m)} - (r_m/r)^6] \quad (3)$$

of two interacting atoms. $-\epsilon$ defines the energy minimum where two non-bonded atoms are r_m apart; α is

the curvature of the function and r is the actual distance between the two atoms. Only pairs of atoms less than 6 Å apart are considered in order to avoid unnecessary calculation times. If atoms come within distances of less than 2.4 Å in case of H...H, C...H, N...H and O...H and 3.0 Å in case of C...C, C...N, C...O, N...O and O...O, Eq. (3) is replaced by $E_{nb} = K/r^4$ where $K = 54.4$ for the first group and 167.5 for the second one. This is done to avoid problems with the attracting part of the Buckingham potential in the case of impossibly short interatomic distances.⁹ The values given for K were selected empirically to give a smooth connection of this function and the potential (3).

On torsion of the exocyclic single bonds by the dihedral angle ϕ the conjugation energy E_π is changed according to Eq. (4). The bond order p_j has to be

$$E_\pi = 247 \cdot p_j^2 \cdot (2 \cos^2 \phi - |\cos^3 \phi|) \quad (4)$$

deduced from a PPP-calculation of the planar conformation; the function contained in the literature²⁵ has been changed in order to get higher sensitivity at torsional angles around 90° and a smoothing at small torsional angles.

Function (5)²⁵ gives the pairwise interaction of permanent dipole moments μ_A and μ_B which are separated by the distance R .

$$E_\mu = 60.24 \frac{\mu_A \cdot \mu_B}{R^3 \cdot DK} \cdot (\cos \chi - 3 \cos \alpha_1 \cdot \cos \alpha_2) \quad (5)$$

χ is the angle between the two moments and α_1 and α_2 are the angles between the moments and the distance vector \vec{R} . The microscopic dielectric constant is given by DK . To use this equation the following assumptions were made. The partial permanent dipole moments are centered at the individual pyrrolic ring systems or in case of attached functional groups at the centers of these groups and are derived from MINDO/3 calculations²⁷ or tables of functional group moments.²⁸

The function used to calculate the hydrogen bonding term E_H is a Buckingham potential (3) which is parameterized accordingly together with function (6) in the case of $r < r_m$

$$E_H = K/r^4 - (K/r_m^4 + \epsilon) \quad (6)$$

3. *The parameters of the functions (2)–(6).* The parameterization of the five functions was done in a stepwise manner. First, values for the parameters of (2) and (3) from the literature^{6,23-25} were adapted on the model compound system (1) (Fig. 1) which was studied experimentally with respect to equilibrium

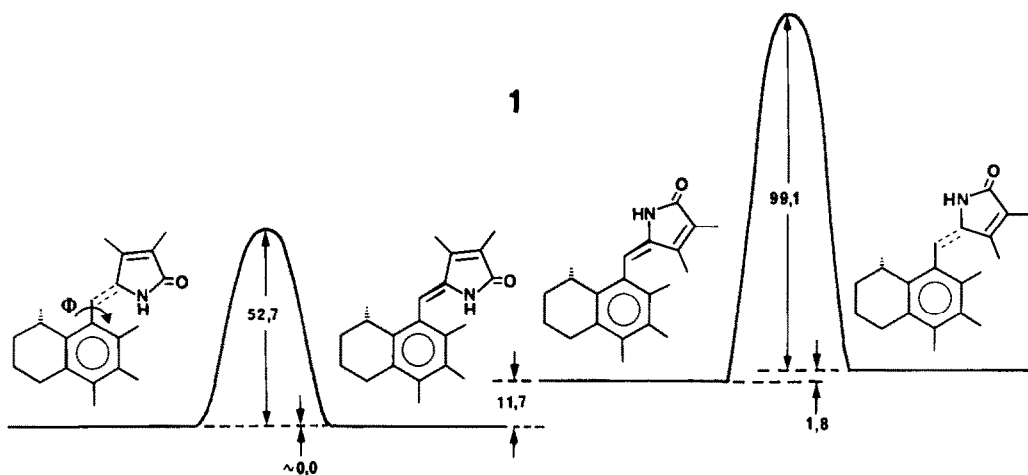


Fig. 1. The model system (1) for the parameterization of functions (2) and (3); energies in kJ mol^{-1} . The left pair of conformers have the *Z* configuration; the right pair are *E*.

and transition energies and ground state geometries for this purpose.²⁹ In this system E_μ and E_H can be neglected as well as E_π due to a nearly perpendicular arrangement at the methine single bond. All energies given in Fig. 1 as well as the geometrical features of **1** were well reproduced ($\pm 1 \text{ kJ mol}^{-1}$, torsional angle $\phi = 90 \pm 5^\circ$) using the K_θ values of 0.038, 0.071 and 0.073 for $\theta = 110^\circ$, 120° and 126° and for the out of plane deformation in Eq. (2). The parameters for Eq. (3) had to be set for the interaction of $\text{H} \dots \text{H}$ to $\epsilon = 0.116 \text{ kJ mol}^{-1}$ at $r_m = 3.20 \text{ \AA}$; for $\text{H} \dots \text{X}$ ($\text{X} = \text{C}, \text{N}, \text{O}$), $\epsilon = 0.087 \text{ kJ mol}^{-1}$ at $r_m = 3.35 \text{ \AA}$; and for $\text{X} \dots \text{X}$, $\epsilon = 0.276 \text{ kJ mol}^{-1}$ at $r_m = 3.85 \text{ \AA}$; α being fixed to 12.0 in all cases to obtain agreement between experimental data²⁹ and force field results.

Second, the only parameter in (4) is the bond order p_{ij} which is determined as mentioned by means of a PPP calculation of a planar conformation.

Third, the permanent partial dipole moments needed for function (5) were calculated for the main pyrrole ring types using the MINDO/3 approximation which yields results⁹ in very satisfactory agreement with experimental data. The pyrrole moiety thereby has a moment of 1.97 D, and for more complex units

the following moments were calculated: 2-methylene-3,4,5-trimethyl-2H-pyrrolyl-, 1.28 D; 5-methylene-3,4-dimethyl-3-pyrroline-2-one fragment, 3.78 D; and 2,3,4-trimethyl-5-hydroxy-2H-pyrrole, 0.65 D. If DK has a value of 2.0 in (5), and the parameters given above for (2), (3) and (4) are used, the experimental details of geometry and energy gained for (*Z*)-3,4-dimethyl-5-(3-bromo-4-methylphenylmethylene)-3-pyrroline-2-one³⁰ were reproduced by the model within 5° and 4 kJ mol^{-1} .

Fourth, for H-bonding systems the experimental data for (*Z*)- and (*E*)-3,4-dimethyl-5-(2-pyridyl)-3-pyrroline-2-one³¹ as well as for pyrromethenes³² were used to parameterize functions (3) and (6). $c = 12.56 \text{ kJ mol}^{-1}$ at $r_m = 1.75 \text{ \AA}$, $\alpha = 12.0$ and $K = 125.6$ at distances $r < r_m$, gave satisfactory results.

As the parameters of Eq. (2)–(6) were derived from experiments on solutions, force field calculations should therefore be able to cope with conformational problems of polypyrrolic compounds in solution.

RESULTS AND DISCUSSIONS

1. Dipyrrolic compounds

Pyrromethenes. The conformational analysis of pyrromethenes, a very important partial structure of

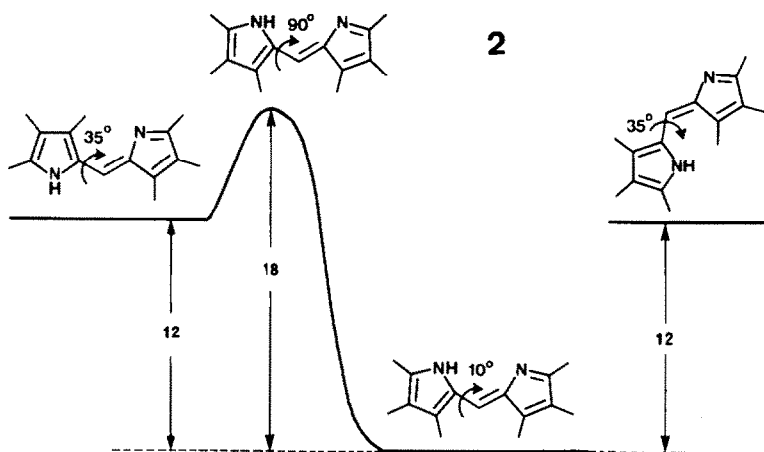


Fig. 2. Force field results on the pyrromethene (2) (kJ mol^{-1}). The diastereomer on the extreme right has the *E* configuration; the other conformers are *Z*.

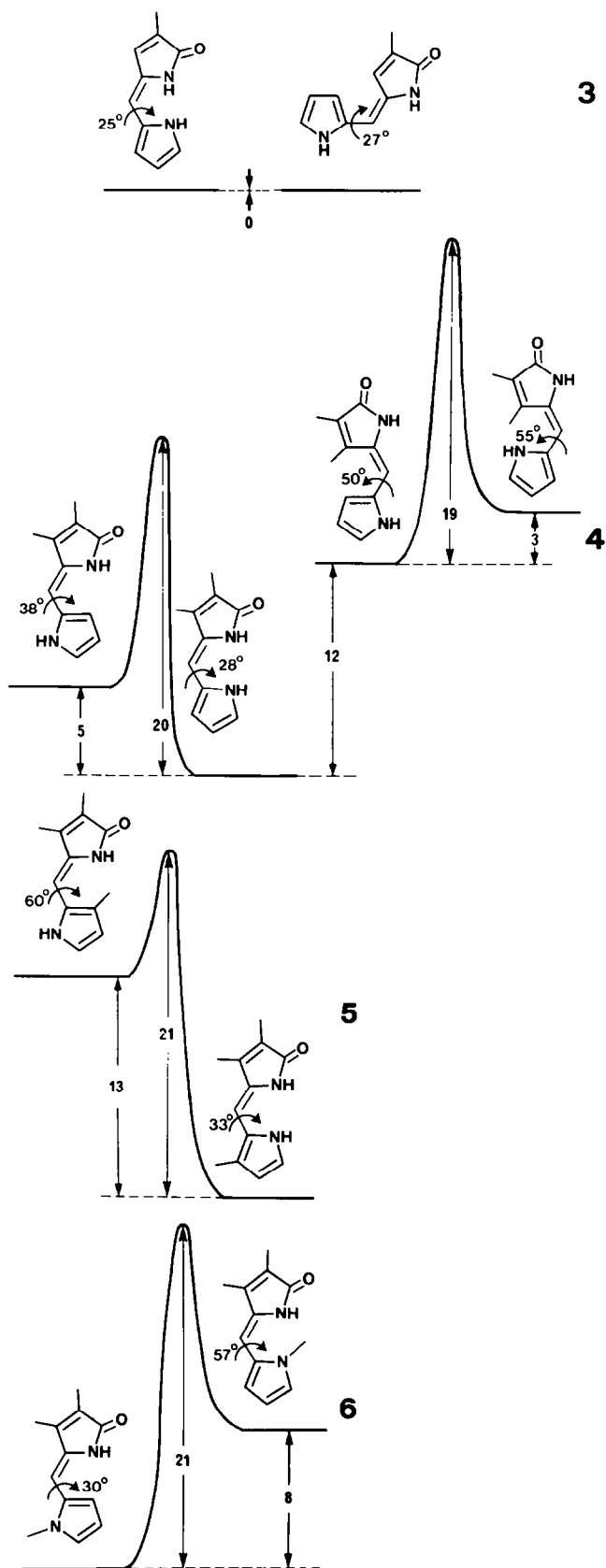


Fig. 3. Force field results on the pyrromethenones (*Z*)- and (*E*)-3; (*Z*) and (*E*)-4, (*Z*)-5 and (*Z*)-6 (kJ mol^{-1}).

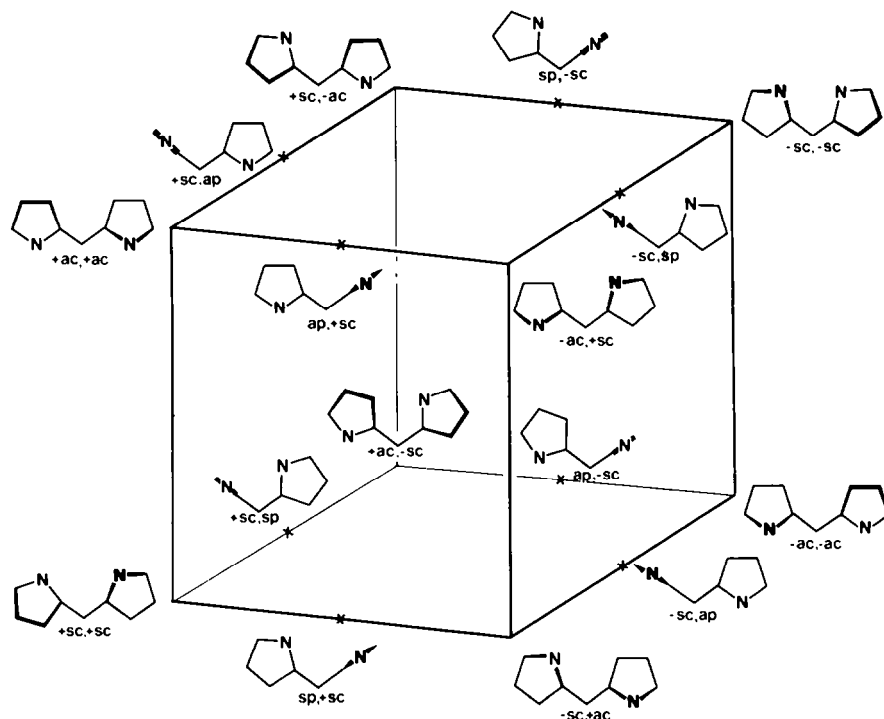


Fig. 4. Diagram for all possible conformers and interconversion paths of an unsymmetrically substituted dipyrromethane ("left" and "right" pyrrole rings are formally distinguished as such). Isomers are identified according to the IUPAC nomenclature of conformations (cf.^{14,34}).

verdinoic bile pigments is summarized in Fig. 2. The results are in agreement with experimental data³² and CNDO/2 calculations.⁷ The stabilization of the (*Z*)-*sp*-conformer* is almost completely due to the intramolecular H-bond.

When both N atoms are methylated the (*Z*)-*sc* conformation with a torsional angle of 65° is the most stable (compare ref. 11a).

Pyromethenones. The results of a conformational analysis of four representative pyromethenones (3–6) which constitute a partial structure of verdinoid and rubinoid bile pigments are given in Fig. 3. Comparison of the *Z/E* pairs of 3 and 4 shows clearly the experimentally well documented³³ effect of an alkyl residue in position 4 of the lactam ring. The energy difference between *Z* and *E* diastereomers stems exclusively from the steric bulkiness of this substituent in position 4 compared to the lactam NH. The stabilization of the *sp* conformer of (*Z*)-4 over the *ac* conformation is mainly due to the dipole-dipole interaction of the two rings. Substitution of the pyrrole ring as in 5 increases this stabilization by the additional non-bonded interaction of this substituent and the methine fragment; on N-alkylation (6) the *ac* conformer becomes the most stable one. All the features of Fig. 3 (except the interconversion barriers which have not so far been measured) are in agreement with experimental conformational analysis³³ regarding geometry as well as energy, and with X-ray crystallographic results^{17,18,34} on monomeric species. Moreover force field calculation on the H-bonded dimer of (*Z*)-4 reveals a flat energy surface ($\pm 1 \text{ kJ mol}^{-1}$) in the region of $0 \pm 20^\circ$

of the two torsional angles. A roughly coplanar dimer has been deduced for dimeric solutions³³ of (*Z*)-4 and the dimers in the crystalline state.^{17,18}

The bond angle deformations found in the calculations of pyromethenes and pyromethenones are in the range of 5–8° in good agreement with X-ray crystallographic values.^{17,18,34}

Dipyrromethanes. These derivatives represent rings B and C of rubinoid bile pigments. The conformational analysis of this structure represents a formidable problem related to the conformational analysis of diarylmethanes which has been discussed explicitly in the literature.³⁵ The various conformers possible, and the isomerization pathways connecting them deduced using methods already described,³⁵ are presented graphically in Fig. 4 for a formally unsymmetrically-substituted dipyrromethane which is, of course, the actual pattern in the natural pigments. The "normal" torsions of the single bonds (β_1, β_2) were defined as 0°, 45°, 90°, ... based on the planar, synperiplanar, synperiplanar (*sp,sp*) conformations. Each corner and the midpoints of the horizontal edges of this graph represent a "special" conformer. Conformers joined by a line through the inversion center of the graph (omitted in Fig. 4 for the sake of clarity) are enantiomeric. Edges at the top and base faces represent so called³⁵ "one ring flips" where the "perpendicular" conformers are transition species between the "helical" conformers. Note that such "flips" represent synchronous rotations of both rings at the single bonds.

The edges connecting the top and base faces are interconversion paths of the "two ring flip" type. Diagonals through the center of the graph (omitted for the sake of clarity in Fig. 4) represent "zero ring flips" which have transition states of coplanar

*For conformational nomenclature see *Pure and Appl. Chem.* **45**, 13 (1976).

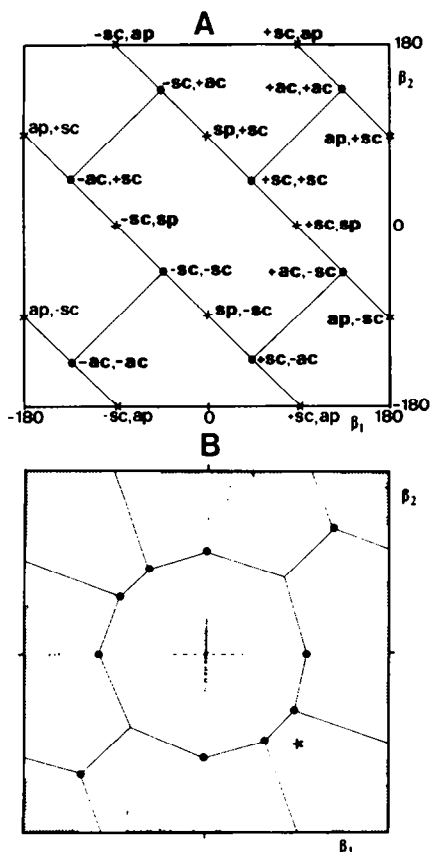


Fig. 5. Conformers (○ ... helical, × ... perpendicular conformations) and interconversion paths ("single and two ring flips") of an unsymmetrically substituted dipyrromethane (A) and energy hypersurface (○ minima, * experimentally found geometry, shaded region $\geq 15 \text{ kJ mol}^{-1}$ above minima) from force field calculations (B).

geometry. Fig. 5 is a transformation of this graph into the conformational space (A) [variables are the two torsional angles β_1 and β_2] which may be compared with the calculated energy hypersurface (B). The minima of this surface are of equal energy within about 1 kJ mol^{-1} . Along the interconversion path barriers up to only about $10\text{--}12 \text{ kJ mol}^{-1}$ have to

be surmounted. "Zero ring flip" (e.g. $+ac, +ac$ to $-ac, -ac$ via ap, ap) interconversions are "forbidden" by the high energies needed.³⁷

It is interesting to note that X-ray crystallography of a dipyrromethane substituted with two ethoxycarbonyl groups in 5 and 5' revealed a structure³⁶ which is indicated in Fig. 5 (B) by an asterisk.

Judged from the extremely flat valley which contains all the low-energy conformers only minor forces may shift the actual geometry of a dipyrromethane in a given state (crystal, solutions). This appears to be the case in the example given above³⁶—an intermolecular hydrogen bonding scheme stabilizes a certain conformation which nevertheless is quite close to the calculated ones. No experimental data on solutions of dipyrromethanes are yet available.

2. Tripyrrolic compounds

We have studied derivatives 7 and 8, which contain a partial structure of the verdinoid bile pigments and the chromophoric unit of the biliviolins.^{31,38,39} The results of calculations are summarized in Fig. 6. In the chelate 7 a destabilization of the *E* derivative by about 15 kJ mol^{-1} is found which compares to an experimental value of about 20 kJ mol^{-1} in ethanol³⁸ and $\geq 25 \text{ kJ mol}^{-1}$ in chloroform. The BF_2 -moiety has been approximated by a CH_2 fragment in the calculations. Obviously BF_2 is somewhat larger than CH_2 as the torsional angles are somewhat smaller than the ones found experimentally.³⁸ Nevertheless the general features of these diastereomers are qualitatively reproduced very well. The torsional angles found for the two tautomers of 8 are in agreement with the range deduced experimentally.^{31,39} The pronounced stabilization of one tautomer arises from the counterbalance of better H-bonding against reduction of conjugation by stronger twisting at the exocyclic single bonds. Although there are experimental hints now⁴⁰ that this is the case, we think care should be exercised in cases of tautomerism where often an extremely efficiently balanced system is found.

3. Tetrapyrrolic compounds

Verdinoid bile pigments. As there is already a wealth of experimental information on the structural aspects of verdinoid bile pigments there is a good opportunity

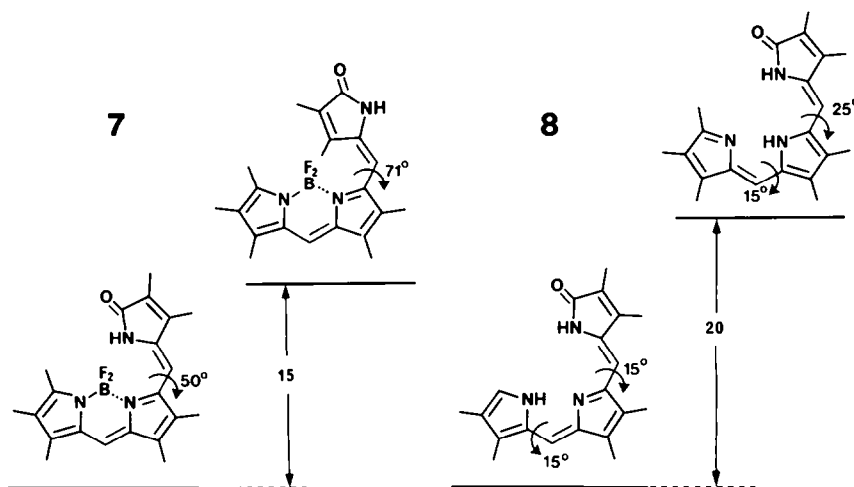


Fig. 6. Force field results on tripyrrolic derivatives (*Z*)- and (*E*)-7 and two tautomers of (*Z*)-8 (kJ mol^{-1}).

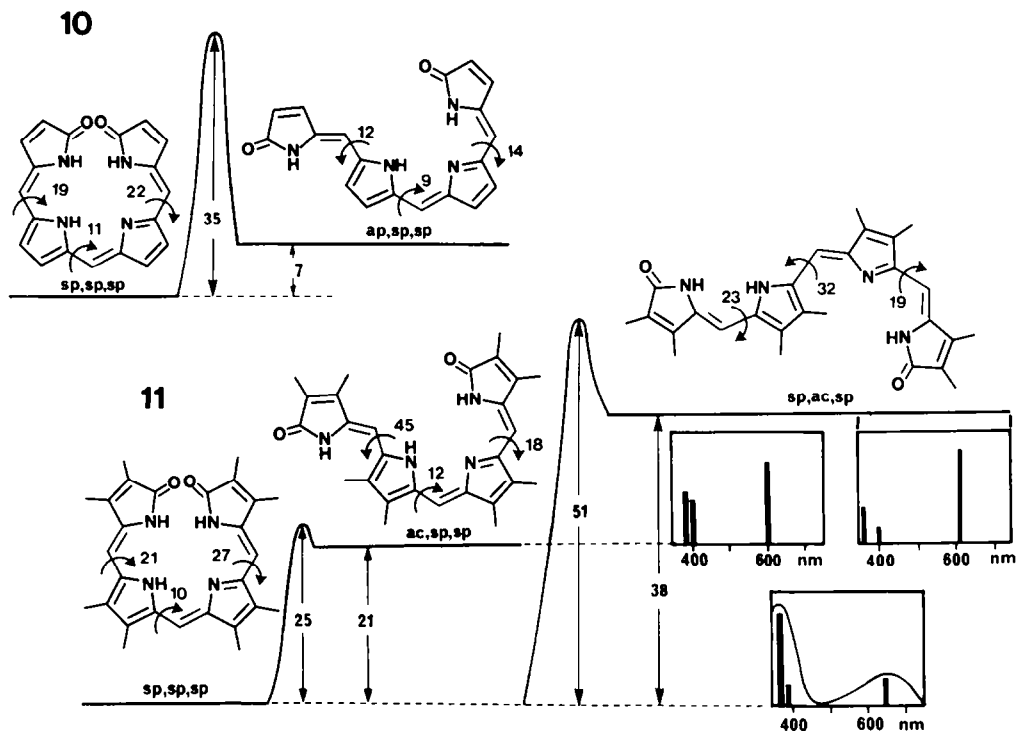
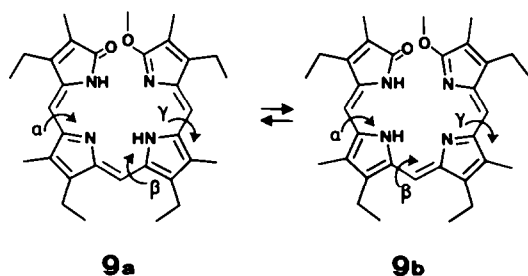


Fig. 7. Conformers in the energetic vicinity of the global minimum for (*Z,Z,Z*)-**10** and **11**. Energies in kJ mol^{-1} , torsional angles in degrees, measured from the planar formulae as it has been drawn. Calculated (PPP) electronic spectra for the three conformers (bars) of **11** and the measured spectrum of **12**.

here to investigate the scope and limitations of the force field model by comparison of calculated and experimental results. One of the best studied molecules, both in solution⁴¹ and in the crystalline state,⁴² is the etiobiliverdin IV γ methyl ether **9**. In the crystalline state **9a** is the predominating tautomer. The torsional angles α , β and γ are found to be 10.4° , 15.8° and 2.5° : there is also some twisting at the exocyclic double bonds.⁴² In solution no differentiation could be made initially⁴¹ between **9a** and **9b**, and we therefore studied a derivative with two methyl groups instead of ethyl groups at the pyromethene fragment (i.e. rings B and C). From NMR coupling data it is possible to deduce that **9a** is also the predominating tautomer in solution.⁴⁰ For both species torsional angles of 25° , 20° and 30° were found by LIS studies.⁴¹

From the force field calculation it is deduced that **9a** is stabilized by about 5 kJ mol^{-1} over **9b** which is an insignificant value for such a large molecule. The torsional angles α , β and γ found are 26° , 15° and 13° for **9a** and 26° , 9° and 20° for **9b**. So, agreement here is very satisfactory, as one has to consider that the



experimental values are, at best, good to $\pm 5^\circ$, and the calculated ones are made somewhat uncertain by a rather flat global energy minimum. The solution structure is clearly reproduced better than is the structure in the crystalline state as the model has been parameterized for the former purpose. On calculation of the absorption spectrum of **9** by the PPP-method (again it has been carefully parameterized²¹) excellent agreement with the measured spectrum⁴¹ is obtained. One therefore may be rather confident about the results of the force field model developed above to yield information on geometry and energy for polypyrrolic systems.

For reasons of comparison we first searched¹³ for the global minimum of the completely unsubstituted bilatriene-*abc* skeleton **10**. It is found to be a helical conformer as depicted in Fig. 7. The corresponding *ap,sp,sp* conformer, which is destabilized only marginally by about 7 kJ mol^{-1} over the *sp,sp,sp* conformer, is separated from the latter by an energy barrier of about 35 kJ mol^{-1} .

Obviously, peripheral alkyl substitution plays an important role in the stabilization of the global minimum as can be seen from Fig. 7 by comparing compounds **10** and **11**. As the substitution of ethyl or propionic acid side chains for methyl groups has only an insignificant impact on the energy hypersurface of the molecule we confine ourselves to permethylated molecules. If one looks for the conformations of ethyl-, vinyl- and propionic side chains they correspond to those found in X-ray crystallographic studies.¹⁷⁻²⁰ On searching for other minima, as depicted in Fig. 7 for **11**, the following could be located (energies above the global minimum in

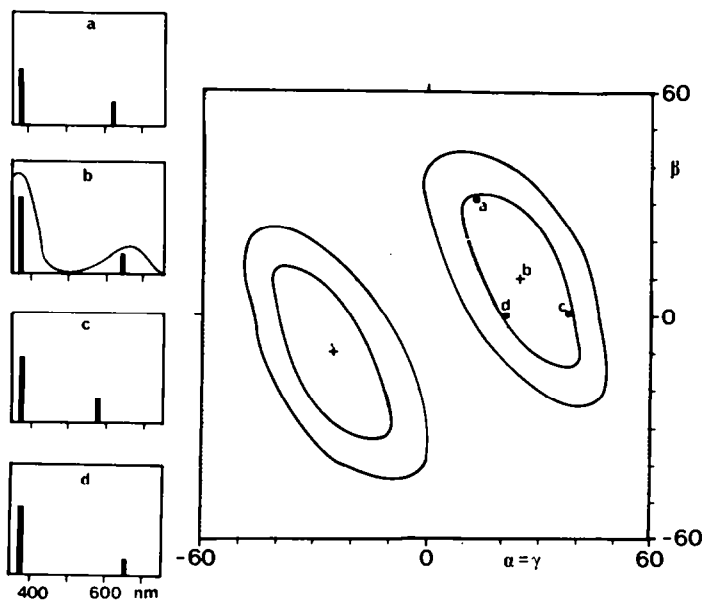


Fig. 8. Energy hypersurface in the vicinity of the enantiomeric global minima of (Z,Z,Z)-(11). Isoenergetic lines are 10 kJ mol^{-1} apart; (+) minima; shaded region 30 kJ mol^{-1} above the minima; (...) trajectories for interconversion of the enantiomeric helices. α , β and γ are the torsional angles as defined in Fig. 7 from left to right. For the points indicated the calculated (PPP, bars) and the measured electronic spectrum (---, CHCl_3) of **12** are included.

kJ mol^{-1} in parentheses): *sp,sp,ac* (25), *ac,sp,ac* (48), *ac,ac,sp* (58), *sp,ac,ac* (63) and *ap,ap,ap* (90), only one enantiomer being considered. These conformers are separated by moderately high energy barriers as can also be seen for the conformers given in Fig. 7.

To obtain a picture of the hypersurface in the vicinity of the global minimum the two torsional angles of the pyrromethenone moieties, α and γ are varied simultaneously by the same values whereas β is the second independent variable. Fig. 8 depicts the result of this process. Two rather extended and shallow valleys contain the global minima corresponding to the enantiomeric helices. Although the actual energy values for the minimum are somewhat lower (as the values for the exact minimum are $\alpha = 21^\circ$, $\beta = 10^\circ$ and $\gamma = 27^\circ$ and not $\alpha = \gamma = 25^\circ$ and $\beta = 10^\circ$), Fig. 8 clearly shows the essential features of the four dimensional surface (α , β , γ , E). The two enantiomers may be interconverted along a trajectory shown in Fig. 8 via a saddle point. The calculated energy for this process amounts to 35 kJ mol^{-1} —in very good agreement with an experimentally determined value⁴³ for ΔG^\ddagger of 42 kJ mol^{-1} at 200 K. Also included in Fig. 8 are the PPP calculations of absorption spectra for some points of the region within 10 kJ mol^{-1} of the global minimum. As any conformation within this area can be easily stabilized by solvation and other external parameters, the absorption spectra may vary accordingly. For example, etiobiliverdin IV γ (**12**; **L14**, $R_2 = R_7 = R_{13} = R_{18} = \text{Me}$, $R_3 = R_8 = R_{12} = R_{17} = \text{Et}$) shows absorption maxima in various solvents at $\lambda_1/\lambda_2 \text{ nm}$ with (ϵ_1/ϵ_2) values of: acetonitrile 635/363 (0.26), methanol 640/364 (0.26), chloroform 635/368 (0.30) pyridine 638/372 (0.32), dimethylsulfoxide 635/371 (0.32) and hexamethylphosphortriamide 625/374 (0.45) with shoulders at 710, 580 and 430 nm. It is seen that the calculated spectra show a variation in λ_1/λ_2

and ϵ_1/ϵ_2 which by comparison with Fig. 7 is not a reliable argument for "open" conformations (e.g. *ac,sp,ac*; *sp,ac,sp*, etc.) compared to "closed" conformations (*sp,sp,sp* to *sc,sc,sc*). Obviously there is a modulation of the hypersurface by external factors as also may be seen in a variable temperature spectrum of this substance (**12**) in 2-methyltetrahydrofuran. At low temperatures (80 K) two bands become discernible in the long wavelength region—one at 640 and one at 690 nm. The latter band is not derived from protonation as has been suggested⁴⁴ in studies of verdins with protic solvents. It might arise by the same sort of stabilization as indicated by chiral solvent induced circular dichroism⁴⁵ or might even come from association. As noted above one should be extremely careful in assigning certain conformational details like "open" or "closed" and "coiled" geometries as there is an ambiguity on the implications of the criteria of relative absorption band intensities or solvent induced circular dichroism. In our opinion there is at present no reliable experimental method which discriminates between, for example, the *ac,sp,sp* and *sc,sp,sc* conformations in solution.

For symmetrically substituted bilatrienes-*abc*, besides the "natural" (Z,Z,Z) isomer, the five diastereomers possessing the configurations (E,Z,Z), (Z,E,Z), (E,Z,E), (E,E,Z) and (E,E,E) are possible. The (Z,Z,Z), (E,Z,Z) and (E,Z,E) have been isolated and characterized in the case of **12**.^{46,47,48} As for unsymmetrically substituted derivatives (e.g. biliverdin) the energetical and geometrical features are not essentially different from those for the symmetrically substituted derivatives we restrict the discussion to the latter. The six diastereomers with their associated energies and geometries of their respective global minima are given in Fig. 9 together with experimental⁴⁸ and calculated electronic spectra of the isomers isolated

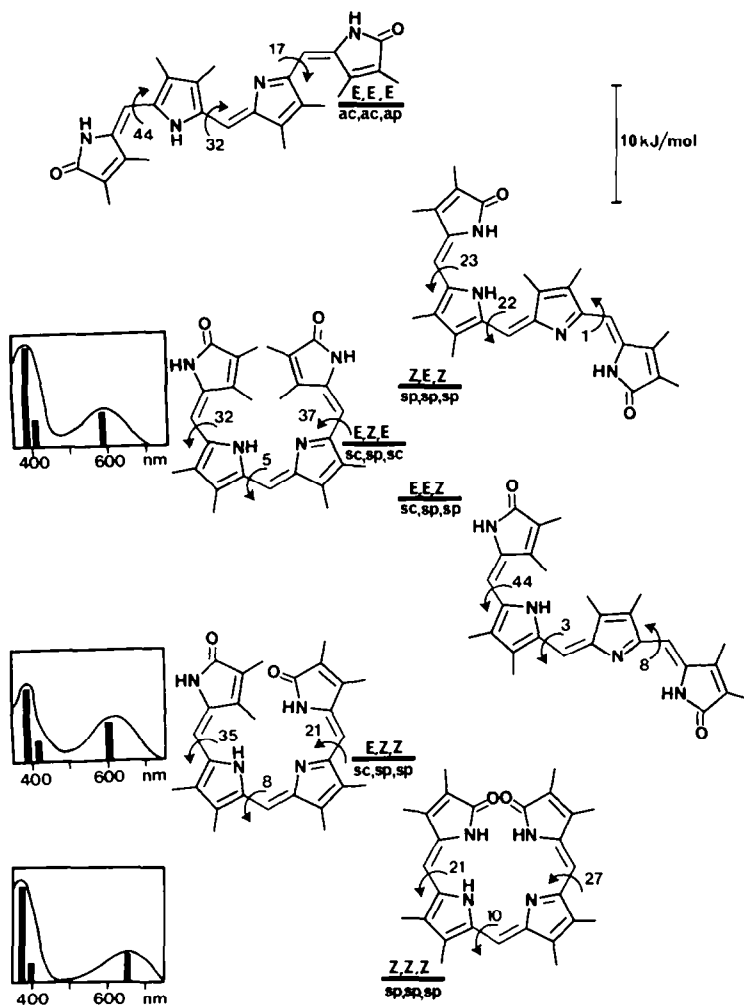


Fig. 9. Family of diastereomers for **11** with calculated (PPP, bars) and experimental electronic spectra (—, CHCl_3) for the given diastereomers of **12**. Torsional angles in degrees; ordered vertically according to their energies.

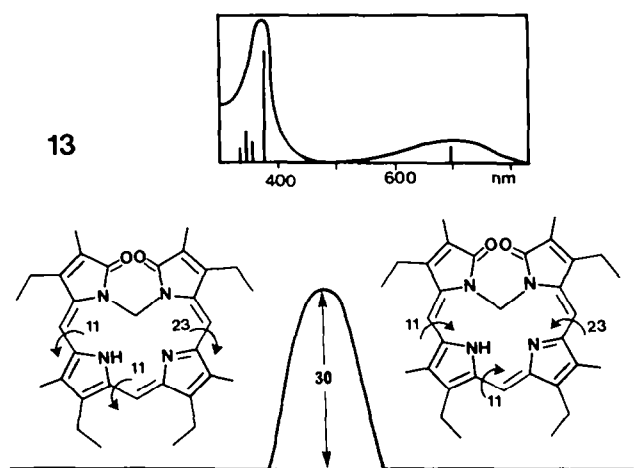


Fig. 10. Geometry and helix interconversion barrier for **13** from force field calculations. Calculated electronic spectrum (PPP, bars) based on these geometrical data and experimental electronic spectrum (—, CHCl_3); torsional angles in degrees.

so far. Good agreement is found for geometrical, spectroscopic and energetic results between model calculations and experimental data.⁴⁶⁻⁴⁹

In general the energetic features and the geometry of bilatrienes-*abc* are determined by non-bonded interactions, especially from the peripheral alkyl substituents, the tendency to remain in a planar conformation stemming from the conjugative term and effective hydrogen bonding.

On N-alkylation of bilatrienes-*abc* the conformational features given above are changed dramatically. The ring A, ring B and ring AD N-methylated derivatives have been investigated experimentally⁵⁰ and by force field calculation¹³ in some detail. These derivatives are much more twisted and a stabilization is observed of diastereomers possessing the *E* configuration at the double bond on the ring bearing the N-methyl group. Of special interest is the N21,N24-bridged derivative **13** (Fig. 10) where the measured free activation enthalpy for helix inversion at 313 K is 60 kJ mol^{-1} and therefore higher than the calculated one (30 kJ mol^{-1}).⁴⁵ The agreement between the electronic spectrum calculated for **13** on the basis of force field geometry ($\alpha = -11^\circ$, $\beta = -11^\circ$, $\gamma = 23^\circ$) and the measured electronic spectrum⁴⁵ is quite good. Nevertheless this case seems to be near the limits of this force field model judged from the comparison of the interconversion energy data.

Rubinoïd bile pigments. On calculating the energy hypersurface of a permethylated biladiene-*ac*¹⁴ it

becomes obvious that this surface is essentially identical with the one found for dipyrromethanes (Fig. 5). The lactam rings attached to the pyrrole rings of the dipyrromethane moiety behave independently. Any stress can easily be relaxed by small torsions of the pyrromethone moieties as was deduced for their partial structures above (Fig. 3). Torsional twisting at the pyrromethone exocyclic single bonds of $15-25^\circ$ are found throughout. Therefore completely alkylated rubinoïd pigments are expected to behave according to the features of the dipyrromethane energy hypersurface, i.e. minor external influences may stabilize one or the other of easily interconverting conformers. An experimental example of such a case may be found in the geometry of bis-*O*-methylbilirubin dimethyl ester which has been found by X-ray crystallography to be a "perpendicular" conformer.²⁰

The substitution of two of the Me groups by propionic acid side chains or the corresponding esters as it is the case in bilirubin (**14**) or bilirubin dimethyl ester (**15**) dramatically changes this picture. For the natural (*4Z,15Z*)-bilirubin a very effective H-bonding system between the lactam rings and the side chains causes two single enantiomeric conformers ($+ac, +ac$ and $-ac, -ac$) to become stabilized with respect to other minima of the energy hypersurface by about 25 kJ mol^{-1} for the dimethyl ester and 35 kJ mol^{-1} for the free diacid as shown in Fig. 11. The geometry of the *ac,ac* conformers closely corresponds to the "ridge tile" geometry found experimentally for bilirubin and its derivatives.⁵¹⁻⁵³ The interconversion barrier between the two enantiomeric conformers via trajectories along the route $+ac, +ac \rightarrow +ac, +sp \rightarrow +ac, -sc \rightarrow +sc, -ac \rightarrow -sp, -ac \rightarrow -ac, -ac$ is calculated to be 30 kJ mol^{-1} for **15** and 45 kJ mol^{-1} for **14**. A free activation enthalpy of about 70 kJ mol^{-1} has been found⁵⁴ for a derivative of **14** which shows that our model still somewhat underestimates the hydrogen bonding potential which governs the "lock-in bonding" of carboxylic side chains and lactam fragments. For non-aqueous solutions it has been found that **14** adopts much the same geometry as in the crystalline state.⁵⁵ The ester (**15**) should be present only as the two enantiomeric conformers when solvated as a monomer.⁵⁶

Calculations on the photoisomers of **14** yield¹⁴ for the (*E,Z*) diastereomer an energy hypersurface exactly as shown in Fig. 11, but 28 kJ mol^{-1} destabilized against the (*Z,Z*) hypersurface with the exception that there is only one H-bonding system possible and accordingly the global minima are only about 26 kJ mol^{-1} below the other minima. For the (*E,E*) diastereomer the energy hypersurface is 62 kJ mol^{-1} above the surface of the (*Z,Z*) diastereomer and it has essentially the same appearance as the one found for peralkylated rubinoïd pigments and dipyrromethanes (compare Fig. 5).

SUMMARY

The force field constructed and parameterized for the conformational analysis of polypyrrolic systems is able to provide information on energies and geometries for linear di-, tri-, and tetra-pyrrolic pigments with high accuracy if one compares the results of the model calculations with those of experiments where they are available. The model thereby serves for a better under-

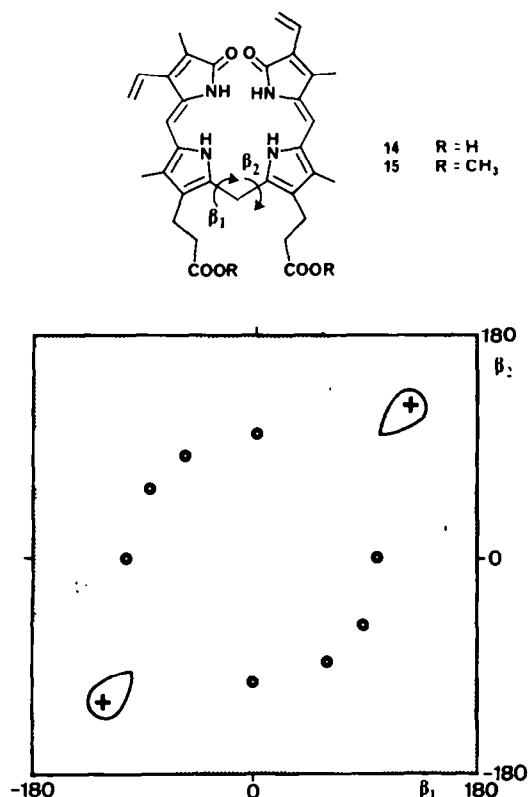


Fig. 11. Energy hypersurface of **14** ($R = H$) and **15** ($R = CH_3$). Shaded regions 15 kJ mol^{-1} above the minima (\circ); (+) global minima 25 kJ mol^{-1} (**15**) and 35 kJ mol^{-1} (**14**) below the contour line (-) corresponding to the values of the other minima (\circ).

standing of structural details (configuration at exocyclic double bonds, substitution, conformation) and their correlation with spectral data for solutions. One can be rather confident about results for species not yet isolated or species which may be invisible to the spectroscopic eye for energetic reasons.

Acknowledgements—The calculations were performed at the computer centres of the Universities of Vienna and Linz, and we are grateful for the generous machine times provided. Thanks are due to the Jubiläumsfonds der Österreichischen Nationalbank for providing funds. We also gratefully acknowledge experimental assistance by Mrs. S. Wansch.

REFERENCES

- ¹R. Schmid and A. F. McDonagh, *The Porphyrins* (Edited by D. Dolphin) Vol. VI, p. 257. Academic Press, New York (1979).
- ²A. Bennett and H. W. Siegelman, *The Porphyrins* (Edited by D. Dolphin) Vol. VI, p. 493. Academic Press, New York (1979).
- ³H. Mohr, *Photomorphogenesis*. Springer, Berlin, 1972.
- ⁴For a recent review see H. Scheer, *Angew. Chem.* **93**, 230 (1981).
- ⁵E.g.: W. T. Borden, *Modern Molecular Orbital Theory for Organic Chemists*. Prentice Hall, New Jersey (1975).
- ⁶S. R. Niketic and K. Rasmussen, *The Self Consistent Force Field*. Springer, Berlin (1977).
- ⁷H. Falk and O. Hofer, *Monatsh. Chem.* **105**, 995 (1974).
- ⁸G. Favini, D. Pitca and P. Manitto, *Nouv. J. Chim.* **3**, 299 (1979).
- ⁹H. Falk, G. Höllbacher, O. Hofer and N. Müller, *Monatsh. Chem.* **112**, 291 (1981).
- ¹⁰A. H. Corwin, J. A. Walter and R. Singh, *J. Org. Chem.* **27**, 4280 (1962).
- ¹¹(a) K. J. Brunings and A. M. Corwin, *J. Am. Chem. Soc.* **64**, 593 (1942); (b) H. Scheer, H. Formanek and W. Rüdiger, *Z. Naturforsch., Teil C* **34**, 1085 (1979).
- ¹²H. Falk, G. Höllbacher and O. Hofer, *Monatsh. Chem.* **110**, 1025 (1979).
- ¹³H. Falk and N. Müller, *Monatsh. Chem.* **112**, 791 (1981).
- ¹⁴H. Falk and N. Müller, *Ibid.* **112**, 1325 (1981).
- ¹⁵N. L. Allinger, *Adv. Phys. Org. Chem.* **13**, 1 (1976).
- ¹⁶QCPE-program Nr. 136.
- ¹⁷D. L. Cullen, P. S. Black, E. F. Meyer, D. A. Lightner, G. D. Quistad and C. S. Pak, *Tetrahedron* **37**, 477 (1977).
- ¹⁸D. L. Cullen, G. Pepe, E. F. Meyer, H. Falk and K. Grubmayr, *J. Chem. Soc. Perkin Trans.* **2**, 999 (1979).
- ¹⁹W. S. Sheldrick, *Ibid.* Perkin Trans. **2**, 1457 (1976).
- ²⁰W. S. Sheldrick and W. Becker, *Z. Naturforsch., Teil B* **34**, 1542 (1979).
- ²¹H. Falk and G. Höllbacher, *Monatsh. Chem.* **109**, 1429 (1978).
- ²²C. A. Crane, IBM program library, 1969.
- ²³N. C. Cohen, *Tetrahedron* **27**, 789 (1971).
- ²⁴E. M. Engler, J. D. Andose and P. v. R. Schleyer, *J. Am. Chem. Soc.* **95**, 8005 (1973); E. Osawa, J. B. Collins and P. v. R. Schleyer, *Tetrahedron* **33**, 2667 (1977).
- ²⁵N. L. Allinger and J. T. Sprague, *J. Am. Chem. Soc.* **95**, 3893 (1973).
- ²⁶J. M. Lehn and G. Ourisson, *Bull. Soc. Chim. France* 1119 (1963).
- ²⁷R. C. Bingham, M. S. Dewar and D. H. Lo, *J. Am. Chem. Soc.* **97**, 1285 (1975); QCPE program No. 279.
- ²⁸A. L. McClellan, *Tables of Experimental Dipole Moments*. Freeman, San Francisco (1963); Vol. 2, Rahara, El Cerrito (1974).
- ²⁹H. Falk, O. Hofer and A. Leodolter, *Monatsh. Chem.* **107**, 907 (1976).
- ³⁰H. Falk and J. M. Ribo, *Ibid.* **107**, 307 (1976).
- ³¹H. Falk and K. Grubmayr, *Ibid.* **108**, 625 (1977).
- ³²H. Falk, S. Gergely and O. Hofer, *Ibid.* **105**, 1004 (1974).
- ³³H. Falk, K. Grubmayr, G. Höllbacher, O. Hofer, A. Leodolter, F. Neufingerl and J. M. Ribo, *Ibid.* **108**, 1113 (1977); H. Falk, K. Grubmayr, U. Herzig and O. Hofer, *Tetrahedron Lett.* 559 (1975).
- ³⁴A. Hori, S. Mangani, G. Pepe, E. F. Meyer, D. L. Cullen, H. Falk and K. Grubmayr, *J. Chem. Soc. Perkin Trans.* **2**, 1525 (1981).
- ³⁵D. Gust and K. Mislow, *J. Am. Chem. Soc.* **95**, 1535 (1973).
- ³⁶R. Bonnett, M. B. Hursthouse and S. Neidle, *J. Chem. Soc. Perkin Trans.* **2**, 1335 (1972).
- ³⁷The energy hypersurface is in principle much the same as the one obtained by CNDO/2-method.⁸ The energies of the "forbidden" regions seem to be somewhat overestimated by the latter method.
- ³⁸H. Falk, K. Grubmayr and F. Neufingerl, *Monatsh. Chem.* **110**, 1127 (1979).
- ³⁹H. Falk, S. Gergely, K. Grubmayr and O. Hofer, *Z. Naturforsch., Teil B* **32**, 299 (1977).
- ⁴⁰H. Falk, K. Grubmayr, K. Magauer, N. Müller and V. Zrunek, *Isr. J. Chem.*, in press.
- ⁴¹H. Falk, K. Grubmayr and K. Thirring, *Z. Naturforsch., Teil B* **33**, 924 (1978).
- ⁴²C. Kratky, C. Jorde, H. Falk and K. Thirring, *Tetrahedron* **39**, 1859 (1983).
- ⁴³H. Lehner, W. Riemer and K. Schaffner, *Justus Liebig's Ann. Chem.* 1798 (1979).
- ⁴⁴C. Petrier, P. Jardon, C. Dupuy and R. Gautron, *J. Chim. phys.* **78**, S 19 (1981); A. R. Holzwarth, H. Lehner, S. E. Braslavsky and K. Schaffner, *Justus Liebig's Ann. Chem.* 2002 (1978).
- ⁴⁵H. Falk and K. Thirring, *Tetrahedron* **37**, 761 (1981).
- ⁴⁶H. Falk, K. Grubmayr, E. Haslinger, T. Schlederer and K. Thirring, *Monatsh. Chem.* **109**, 1451 (1978).
- ⁴⁷H. Falk and K. Grubmayr, *Angew. Chem.* **89**, 487 (1977).
- ⁴⁸H. Falk, N. Müller and T. Schlederer, *Monatsh. Chem.* **111**, 159 (1980).
- ⁴⁹H. Falk and K. Grubmayr, *Ibid.* **110**, 1237 (1979).
- ⁵⁰H. Falk and K. Thirring, *Z. Naturforsch., Teil B* **34**, 1448, 1600 (1979); **35**, 376 (1980).
- ⁵¹R. Bonnett, J. E. Davies and M. B. Hursthouse, *Nature, London* **262**, 326 (1976).
- ⁵²G. LeBas, A. Allegret, Y. Manguen, C. DeRango and M. Bailly, *Acta Crystallogr.* **B36**, 3007 (1980).
- ⁵³A. Mugnoli, P. Manitto and D. Monti, *Nature, London* **273**, 568 (1978).
- ⁵⁴P. Manitto and D. Monti, *J. Chem. Soc. Chem. Commun.* 122 (1976).
- ⁵⁵D. Kaplan and G. Navon, *Ibid.* Perkin Trans. **2**, 1374 (1981).
- ⁵⁶Cf. H. Falk and N. Müller, *Monatsh. Chem.* **113**, 11 (1982).